

State-independent quantum contextuality with single photons

Elias Amsellem,¹ Magnus Rådmark,¹ Mohamed Bourennane,¹ and Adán Cabello²

¹*Department of Physics, Stockholm University, S-10691, Stockholm, Sweden*

²*Departamento de Física Aplicada II, Universidad de Sevilla, E-41012 Sevilla, Spain*

(Dated: August 29, 2018)

We present an experimental state-independent violation of an inequality for noncontextual theories on single particles. We show that 20 different single-photon states violate an inequality which involves correlations between results of sequential compatible measurements by at least 419 standard deviations. Our results show that, for any physical system, even for a single system, and independent of its state, there is a universal set of tests whose results do not admit a noncontextual interpretation. This sheds new light on the role of quantum mechanics in quantum information processing.

PACS numbers: 03.65.Ta, 03.65.Ud, 42.50.Xa

The debate on whether quantum mechanics can be completed with hidden variables started in 1935 with an ingenious example proposed by Einstein, Podolsky, and Rosen [1] (EPR), suggesting that quantum mechanics only gives an incomplete description of nature. Schrödinger pointed out the fundamental role of quantum entanglement in EPR's example and concluded that entanglement is “the characteristic trait of quantum mechanics” [2]. For years, this has been a commonly accepted paradigm, stimulated by the impact of the applications of entanglement in quantum communication [3, 4], quantum computation [5], and violations of Bell inequalities [6, 7, 8, 9, 10, 11, 12, 13]. However, Bohr argued that similar paradoxical examples occur every time we compare different experimental arrangements, without the need of entanglement nor composite systems [14]. The Kochen-Specker (KS) theorem [15, 16, 17] illustrates Bohr's intuition with great precision. The KS theorem states that, for every physical system there is always a finite set of tests such that it is impossible to assign them predefined noncontextual results in agreement with the predictions of quantum mechanics [15, 17]. Remarkably, the proof of the KS theorem [17] requires neither a composite system nor any special quantum state: it holds for any physical system with more than two internal levels (otherwise the notion of noncontextuality becomes trivial), independent of its state. It has been discussed for a long time whether or not the KS theorem can be translated into experiments [18, 19]. Recently, however, quantum contextuality has been tested with single photons [20, 21] and single neutrons [22] in specific states.

Very recently it has been shown that the KS theorem can be converted into experimentally testable state-dependent [23] and state-independent [24] violations of inequalities involving correlations between compatible measurements. For single systems, only a state-dependent violation for a specific state of single neutrons has been reported [25]. A state-independent violation has been observed only in composite systems of two $^{40}\text{Ca}^+$ trapped ions [26]. Following the spirit of the original KS theorem, which deals with the problem of

hidden variables in single systems, we report the first state-independent violation for single-particle systems.

Any theory in which the nine observables $A, B, C, a, b, c, \alpha, \beta$, and γ have predefined noncontextual outcomes -1 or $+1$, must satisfy the following inequality [24]:

$$\chi \equiv \langle ABC \rangle + \langle abc \rangle + \langle \alpha\beta\gamma \rangle + \langle Aa\alpha \rangle + \langle Bb\beta \rangle - \langle Cc\gamma \rangle \leq 4, \quad (1)$$

where $\langle ABC \rangle$ denotes the ensemble average of the product of the three outcomes of measuring the mutually compatible observables A , B , and C . Surprisingly, for any four-dimensional system, there is a set of observables for which the prediction of quantum mechanics is $\chi = 6$ for any quantum state of the system [24]. The purpose of this experiment is to test this prediction on different quantum states of a single-particle system.

A physical system particularly well suited for this purpose is the one comprising a single photon carrying two qubits of quantum information: the first qubit is encoded in the spatial path s of the photon, and the second qubit in the polarization p . The quantum states $|0\rangle_s = |t\rangle_s$ and $|1\rangle_s = |r\rangle_s$, where t and r denote the transmitted and reflected paths of the photon, respectively, provide a basis for describing any quantum state of the photon's spatial path. Similarly, $|0\rangle_p = |H\rangle_p$ and $|1\rangle_p = |V\rangle_p$, where H and V denote horizontal and vertical polarization, respectively, provide a basis for describing any quantum state of the photon's polarization.

A suitable choice of observables giving $\chi = 6$ is the following [24]:

$$\begin{aligned} A &= \sigma_z^s, & B &= \sigma_z^p, & C &= \sigma_z^s \otimes \sigma_z^p, \\ a &= \sigma_x^p, & b &= \sigma_x^s, & c &= \sigma_x^s \otimes \sigma_x^p, \\ \alpha &= \sigma_z^s \otimes \sigma_x^p, & \beta &= \sigma_x^s \otimes \sigma_z^p, & \gamma &= \sigma_y^s \otimes \sigma_y^p, \end{aligned} \quad (2)$$

where σ_z^s denotes the Pauli matrix along the z direction of the spatial path qubit, σ_x^p denotes the Pauli matrix along the x direction of the polarization qubit, and \otimes denotes tensor product.

To generate polarization-spatial path encoded single-photon states, we used the setup described in Fig. 1. We

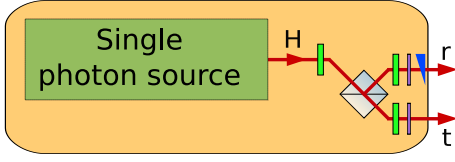


FIG. 1: Preparation of the polarization-spatial path encoded states of single photons. The setup consists of a source of H -polarized single photons followed by a half wave plate (HWP) and a polarizing beam splitter (PBS), allowing any probability distribution of a photon in the paths t and r . The wedge (W) placed in one of the paths adds an arbitrary phase shift between both paths. A HWP and a quarter wave plate (QWP) in each path allow us to rotate the outputs of the PBS to any polarization. Symbol definitions are given at the bottom of Fig. 2.

experimentally tested the value of χ for 20 different quantum states. It is of utmost importance for the experiment that the measurements of each of the nine observables in (2) are context independent [24], in the sense that the measurement device used for the measurement of, e.g., B must be the same when B is measured with the compatible observables A and C , and when B is measured with b and β , which are compatible with B but not with A and C . For the experiment we used the measurement devices described in Fig. 2, which satisfy this requirement.

For a sequential measurement of three compatible observables on the same photon, we used the single-observable measuring devices in Fig. 2, appropriately arranged as described in Fig. 3. Since the predictions of both noncontextual hidden variable theories and quantum mechanics do not depend on the order of the compatible measurements, we chose the most convenient order for each set of observables (e.g., we measured CBA instead of ABC). This was usually the configuration which minimized the number of required interferometers and hence maximized the visibility. Specifically, we measured the averages $\langle CAB \rangle$, $\langle cba \rangle$, $\langle \beta\gamma\alpha \rangle$, $\langle \alpha Aa \rangle$, $\langle \beta bB \rangle$, and $\langle c\gamma C \rangle$, as described in Fig. 3.

Our single-photon source was an attenuated stabilized narrow bandwidth diode laser emitting at 780 nm and offering a long coherence length. The laser was attenuated so that the two-photon coincidences were negligible. The mean photon number per time window was 0.058.

All the interferometers in the experimental setup are based on free space displaced Sagnac interferometers, which possess a very high stability. We have reached a visibility above 99% for phase insensitive interferometers, and a visibility ranging between 90% and 95% for phase sensitive interferometers.

Our single-photon detectors were Silicon avalanche photodiodes calibrated to have the same detection efficiency. All single counts were registered using an eight-channel coincidence logic with a time window of 1.7 ns.

To test the prediction of a state-independent violation,

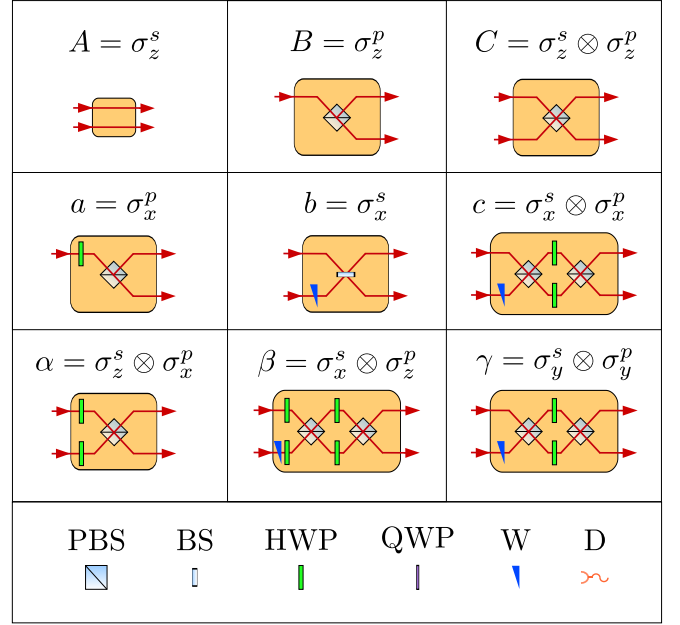


FIG. 2: Devices for measuring the nine observables (2). A measurement of A requires only to distinguish between paths t and r . For measuring b , note that its eigenstates are $(|t\rangle \pm |r\rangle)/\sqrt{2}$ and they need to be mapped to the paths t and r ; this is accomplished by interference with the help of an additional 50/50 beam splitter (BS) and a wedge. The measurements of a and B are standard polarization measurements using a PBS and a HWP. Observables C , c , α , β , and γ are the product of a spatial path and a polarization observable $\sigma_i^s \otimes \sigma_j^p$. Each of these observables has a four-dimensional eigenspace, but since the observables need to be rowwise and columnwise compatible, only their common eigenstates can be used for distinguishing the eigenvalues. This implies that C , c , and γ can be implemented as Bell measurements with different distributions of the Bell states. Similarly, α and β are Bell measurements preceded by a polarization rotation. In this way γ is compatible also with α and β .

we repeated the experiment on 20 quantum states of different purity and entanglement. For each pure state, we checked each of the six correlations in inequality (1) for about 1.7×10^7 photons. The results for the mixed states were obtained by suitably combining pure state data. Fig. 4 shows that a state-independent violation of inequality $\chi \leq 4$ occurs, with an average value for χ of 5.4521. Because of experimental imperfections, the experimental violation of the inequality falls short of the quantum-mechanical prediction for an ideal experiment ($\chi = 6$).

The main systematic error source was due to the large number of optical interferometers involved in the measurements, the nonperfect overlapping of the light modes and the polarization components. The errors were deduced from propagated Poissonian counting statistics of the raw detection events. The number of detected photons was about 1.7×10^6 per second. The measurement

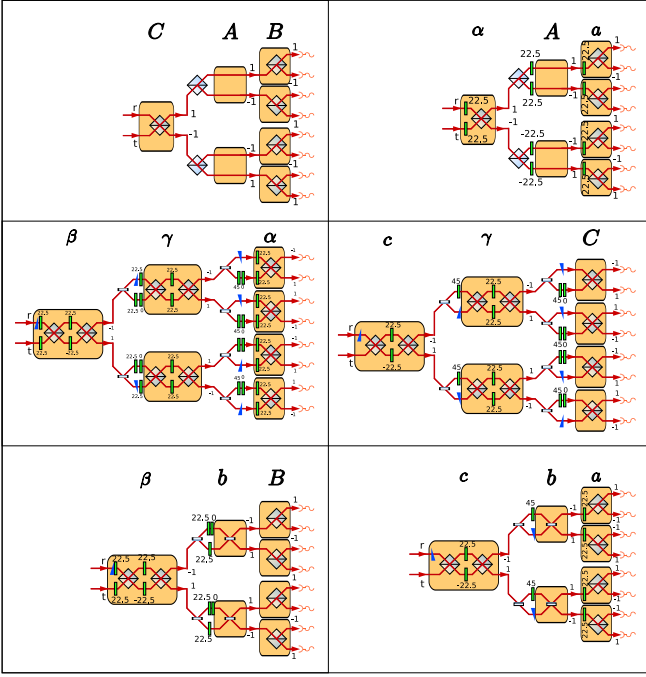


FIG. 3: Setups for measuring the six sets of observables to test inequality (1). We explicitly describe the setup for measuring C , A , and B ; the description of the other setups is obtained by replacing C , A , and B with the corresponding observables. The seven boxes are single-observable measuring devices (see Fig. 2). The photon, prepared in a specific state, enters the device for measuring C through the device's input and follows one of the two possible outcomes. A detection of the photon in one of these outputs would make the measurement of the next observable impossible. Instead, we placed, after each of the two outputs of the C -measuring device, a device for measuring the second observable, A (we thus used two identical A -measuring devices). Similarly, we also placed, after each of the four outputs of the A -measuring devices, a device for measuring the third observable, B (we thus used four identical B -measuring devices). Note that we need to recreate the eigenstates of the measured observable before entering the next observable, since our single-observable measuring devices map eigenstates to a fixed spatial path and polarization. Finally, we placed a single-photon detector (D) after each of the eight outputs of the four B -measuring devices. An individual photon passing through the whole arrangement is detected only by one of the eight detectors, which indicates which one of the eight combinations of results for C , A , and B is obtained.

time for each of the six sets of observables was 10 s for each state.

In Fig. 5 we also present measurement results for each experimental setup for the maximally entangled state $|\psi_3\rangle$ and the product state $|\psi_{14}\rangle$ defined in Table I. Probabilities for each outcome as well as values of the correlations are shown. The overall detection efficiency of the experiment, defined as the ratio of detected to prepared photons, was $\eta = 0.50$. This value was obtained considering that the detection efficiency of the single-photon

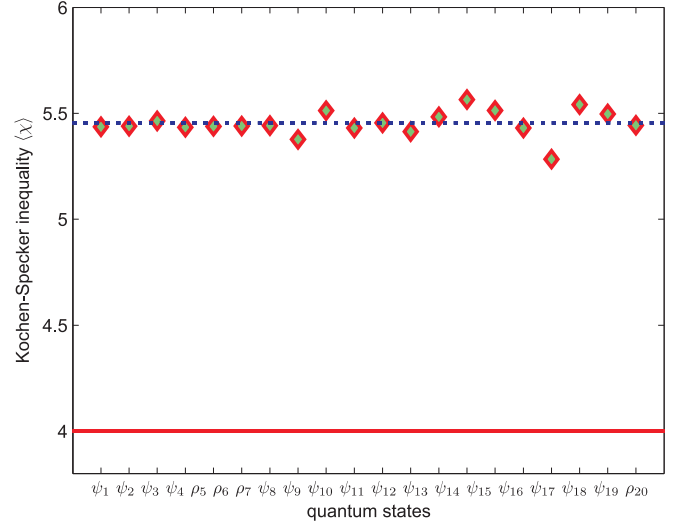


FIG. 4: State independence of the violation of the inequality $\chi \leq 4$. The value of χ was tested for 20 different quantum states: four pure states with maximum internal entanglement between the spatial path and polarization which would maximally violate a Clauser-Horne-Shimony-Holt-Bell-like inequality [27] (states $|\psi_1\rangle$ – $|\psi_4\rangle$), one mixed state with partial internal entanglement which would violate a Clauser-Horne-Shimony-Holt-Bell-like inequality (ρ_5), one mixed state with partial internal entanglement which would not violate a Clauser-Horne-Shimony-Holt-Bell-like inequality (ρ_6), one mixed state without internal entanglement according to the Peres-Horodecki criterion [28, 29] (ρ_7), 12 pure states without internal entanglement ($|\psi_8\rangle$ – $|\psi_{19}\rangle$), and a maximally mixed state (ρ_{20}). The explicit expression of each state is given in Table I. The red solid line indicates the classical upper bound. The blue dashed line at 5.4550 indicates the average value of χ over all the 16 pure states.

detectors is 55% and the fiber coupling is 90%. Therefore, the fair sampling assumption (i.e., the assumption that detected photons are an unbiased subensemble of the prepared photons) is needed to conclude a violation of the inequality. This is the same assumption as is adopted in all previous state-dependent experimental violations of classical inequalities with photons [7, 8, 9, 11, 13, 20, 21] and neutrons [22, 25].

In conclusion, our results show that experimentally observed outcomes of measurements on single photons cannot be described by noncontextual models. A remarkable feature of this experiment is that the quantum violation of a classical inequality requires neither entangled states nor composite systems. It occurs even for single systems which cannot have entanglement. Further on, it occurs for any quantum state, even for maximally mixed states, like ρ_{20} in Fig. 4, which are usually considered “classical” states. This shows that entanglement is not the only essence of quantum mechanics which distinguishes the theory from classical physics; consequently, entanglement might not be the only resource for quantum information processing. Quantum contextuality of single

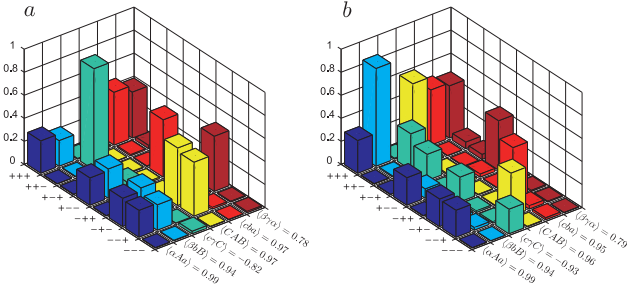


FIG. 5: Correlation measurements of all terms in the inequality (1) for the states $|\psi_3\rangle$ (a) and $|\psi_{14}\rangle$ (b). The figures show experimentally estimated probabilities for detecting a photon in each of the eight detectors. A photon detection corresponds to certain values (± 1) for the three measured dichotomic observables. For example, the bar height at $(+++; \alpha A a)$ represents the probability to obtain the results $\alpha, A, a = +1$, and similarly $(++-; \alpha A a)$ represents $\alpha, A = +1$ and $a = -1$. The expectation values for each measurement are also given.

quantum systems submitted to a sequence of compatible measurements might be an equally powerful, simpler and more fundamental resource.

We thank Y. Hasegawa and J.-Å. Larsson for comments, and acknowledge support by the Swedish Research Council (VR), the Spanish MCI Project No. FIS2008-05596, and the Junta de Andalucía Excellence Project No. P06-FQM-02243.

- [1] A. Einstein, B. Podolsky, and N. Rosen, Phys. Rev. **47**, 777 (1935).
- [2] E. Schrödinger, Proc. Cambridge Philos. Soc. **31**, 555 (1935).
- [3] C. H. Bennett and S. J. Wiesner, Phys. Rev. Lett. **69**, 2881 (1992).
- [4] C. H. Bennett *et al.*, Phys. Rev. Lett. **70**, 1895 (1993).
- [5] R. Raussendorf and H. J. Briegel, Phys. Rev. Lett. **86**, 5188 (2001).
- [6] J. S. Bell, Physics (Long Island City, N.Y.) **1**, 195 (1964).
- [7] A. Aspect, J. Dalibard, and G. Roger, Phys. Rev. Lett. **49**, 1804 (1982).
- [8] W. Tittel, J. Brendel, H. Zbinden, and N. Gisin, Phys. Rev. Lett. **81**, 3563 (1998).
- [9] G. Weihs *et al.*, Phys. Rev. Lett. **81**, 5039 (1998).
- [10] M. A. Rowe *et al.*, Nature (London) **409**, 791 (2001).
- [11] S. Gröblacher *et al.*, Nature (London) **446**, 871 (2007).
- [12] C. Branciard *et al.*, Nat. Phys. **4**, 681 (2008).
- [13] D. N. Matsukevich *et al.*, Phys. Rev. Lett. **100**, 150404 (2008).
- [14] N. Bohr, Phys. Rev. **48**, 696 (1935).
- [15] E. Specker, Dialectica **14**, 239 (1960).

- [16] J. S. Bell, Rev. Mod. Phys. **38**, 447 (1966).
- [17] S. Kochen and E. P. Specker, J. Math. Mech. **17**, 59 (1967).
- [18] A. Cabello and G. García-Alcaine, Phys. Rev. Lett. **80**, 1797 (1998).
- [19] D. A. Meyer, Phys. Rev. Lett. **83**, 3751 (1999).
- [20] C. Simon, M. Żukowski, H. Weinfurter, and A. Zeilinger, Phys. Rev. Lett. **85**, 1783 (2000).
- [21] Y.-F. Huang *et al.*, Phys. Rev. Lett. **90**, 250401 (2003).
- [22] Y. Hasegawa *et al.*, Nature (London) **425**, 45 (2003).
- [23] A. Cabello, S. Filipp, H. Rauch, and Y. Hasegawa, Phys. Rev. Lett. **100**, 130404 (2008).
- [24] A. Cabello, Phys. Rev. Lett. **101**, 210401 (2008).
- [25] H. Bartosik *et al.*, Phys. Rev. Lett. **103**, 040403 (2009).
- [26] G. Kirchmair *et al.*, Nature (London) **460**, 494 (2009).
- [27] J. F. Clauser, M. A. Horne, A. Shimony, and R. A. Holt, Phys. Rev. Lett. **23**, 880 (1969).
- [28] A. Peres, Phys. Rev. Lett. **77**, 1413 (1996).
- [29] M. Horodecki, P. Horodecki, and R. Horodecki, Phys. Lett. A **223**, 1 (1996).

TABLE I: Experimental values of $\langle CAB \rangle + \langle cba \rangle + \langle \beta\gamma\alpha \rangle + \langle \alpha Aa \rangle + \langle \beta bB \rangle - \langle c\gamma C \rangle$ for 20 quantum states. The average value is 5.4550 ± 0.0006 and on average we violate the inequality with 655 standard deviations (SDs).

State	Expectation value	SD
$ \psi_1\rangle = \frac{1}{\sqrt{2}}(t\rangle H\rangle + r\rangle V\rangle)$	5.4366 ± 0.0012	1169
$ \psi_2\rangle = \frac{1}{\sqrt{2}}(t\rangle H\rangle - r\rangle V\rangle)$	5.4393 ± 0.0023	621
$ \psi_3\rangle = \frac{1}{\sqrt{2}}(t\rangle V\rangle + r\rangle H\rangle)$	5.4644 ± 0.0029	498
$ \psi_4\rangle = \frac{1}{\sqrt{2}}(t\rangle V\rangle - r\rangle H\rangle)$	5.4343 ± 0.0026	561
$\rho_5 = \frac{13}{16} \psi_1\rangle\langle\psi_1 + \frac{1}{16}\sum_{j=2}^4 \psi_j\rangle\langle\psi_j $	5.4384 ± 0.0010	1386
$\rho_6 = \frac{5}{8} \psi_1\rangle\langle\psi_1 + \frac{1}{8}\sum_{j=2}^4 \psi_j\rangle\langle\psi_j $	5.4401 ± 0.0010	1509
$\rho_7 = \frac{7}{16} \psi_1\rangle\langle\psi_1 + \frac{3}{16}\sum_{j=2}^4 \psi_j\rangle\langle\psi_j $	5.4419 ± 0.0010	1433
$ \psi_8\rangle = t\rangle H\rangle$	5.3774 ± 0.0020	676
$ \psi_9\rangle = t\rangle V\rangle$	5.5131 ± 0.0032	475
$ \psi_{10}\rangle = r\rangle H\rangle$	5.4306 ± 0.0031	465
$ \psi_{11}\rangle = r\rangle V\rangle$	5.4554 ± 0.0017	850
$ \psi_{12}\rangle = \frac{1}{\sqrt{2}} t\rangle(H\rangle + V\rangle)$	5.4139 ± 0.0015	960
$ \psi_{13}\rangle = \frac{1}{\sqrt{2}} t\rangle(H\rangle + i V\rangle)$	5.4835 ± 0.0022	667
$ \psi_{14}\rangle = \frac{1}{\sqrt{2}}(t\rangle + r\rangle) H\rangle$	5.5652 ± 0.0032	489
$ \psi_{15}\rangle = \frac{1}{\sqrt{2}}(t\rangle + i r\rangle) H\rangle$	5.5137 ± 0.0036	419
$ \psi_{16}\rangle = \frac{1}{2}(t\rangle + r\rangle)(H\rangle + V\rangle)$	5.4304 ± 0.0014	1029
$ \psi_{17}\rangle = \frac{1}{2}(t\rangle + i r\rangle)(H\rangle + V\rangle)$	5.2834 ± 0.0019	674
$ \psi_{18}\rangle = \frac{1}{2}(t\rangle + r\rangle)(H\rangle + i V\rangle)$	5.5412 ± 0.0032	475
$ \psi_{19}\rangle = \frac{1}{2}(t\rangle + i r\rangle)(H\rangle + i V\rangle)$	5.4968 ± 0.0032	462
$\rho_{20} = \frac{1}{4}\sum_{j=1}^4 \psi_j\rangle\langle\psi_j $	5.4437 ± 0.0012	1229